ACS APPLIED MATERIALS & INTERFACES

Research Article

www.acsami.org

$(K,Na)NbO_3$ Nanofiber-based Self-Powered Sensors for Accurate Detection of Dynamic Strain

Zhao Wang,[†] Youdong Zhang,[†] Shulin Yang,[†] Yongming Hu,[†] Shengfu Wang,[†] Haoshuang Gu,*[,†] Yu Wang,*[,‡] H. L. W. Chan,[‡] and John Wang[§]

[†]Hubei Collaborative Innovation Centre for Advanced Organic Chemical Materials, Faculty of Physics and Electronic Science, College of Chemistry & Chemical Engineering, Hubei University, Wuhan, Hubei Province People's Republic of China

[‡]Department of Applied Physics and Materials Research Centre, The Hong Kong Polytechnic University, Hong Kong SAR, People's Republic of China

[§]Department of Materials Science and Engineering, Faculty of Engineering, National University of Singapore, Singapore 117574, Singapore

Supporting Information

ABSTRACT: A self-powered active strain sensor based on well-aligned $(K,Na)NbO_3$ piezoelectric nanofibers is successfully fabricated through the electrospinning and polymer packaging process. The device exhibits a fast, active response to dynamic strain by generating impulsive voltage signal that is dependent on the amplitude of the dynamic strains and the vibration frequency. When the frequency is fixed at 1 Hz, the peak to peak value of the voltage increases from ~1 to ~40 mV, and the strain changes from 1 to 6%. Furthermore, the output voltage is linearly increased by an order of magnitude with the frequency changing from 0.2 to 5 Hz under the same strain amplitude. The influence of frequency on the output voltage can be further enhanced at higher strain amplitude. This phenomenon is attributed to the increased generating rate of piezoelectric charges under higher strain rate of the nanofibers. By counting the pulse separation of the voltage peaks, the vibration frequency is synchronously measured during the sensing process. The accuracy of the sensing results can be improved by calibration according to the frequency-dependent sensing behavior.

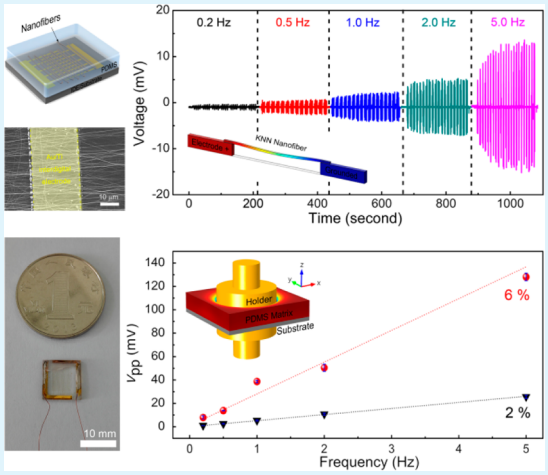

KEYWORDS: *$(K,Na)NbO_3$, nanofibers, piezoelectric, active sensor, dynamic strain*

1. INTRODUCTION

Recently, new strain sensors have been widely explored for accurately measuring deformation, force, moment, pressure, weight, and acceleration in many fields.[1−5] Due to the rapid development of smart and wireless sensor networks, the sensors are required to miniaturize for integration.[6,7] Until now, most of the microscaled strain sensors are actually transducers that convert the mechanical energy into electrical signals. This process is realized by using either piezoresistive or piezoelectric nanomaterials.[8,9] Although the piezoresistive strain sensors have been widely used, these devices still require power sources, such as a Li-ion battery, which actually limits the miniaturization and long-term performance of the system. Therefore, an investigation into the self-powered strain sensor microsystems has attracted the attention of many researchers.

Other than the passive piezoresistive materials, energy harvesters based on piezoelectric nanowires can be employed for active sensing of dynamic strains by generating output voltage or current signals depending on the strain of nanowires. Because the electrical signal used for the sensing operation is generated through the piezoelectric energy harvesting process of the nanowires, the sensors are self-powered and can operate without external electrical power units. For example, sensors based on ZnO piezoelectric nanowires have been used to detect movement, the pressure of rotating tires, and the vibration of drum membrane by means of the peak value of the output voltage/current signals.[10−17] Because the sensitivity of active sensors is largely determined by the electromechanical conversion efficiency of the nanowires, the relatively low piezoelectric voltage constant of ZnO nanowires may limit the output voltage and sensitivity of the devices. In contrast, $(K,Na)NbO_3$ (KNN) materials are regarded as an excellent candidate for building piezoelectric energy harvesters due to the relatively higher piezoelectric voltage constant near the morphotropic phase boundary.[18,19] For example, Kanno and coauthors reported that the performance of energy harvester

Received: December 21, 2014
Accepted: February 9, 2015
Published: February 9, 2015

DOI: 10.1021/am5090012
ACS Appl. Mater. Interfaces 2015, 7, 4921−4927

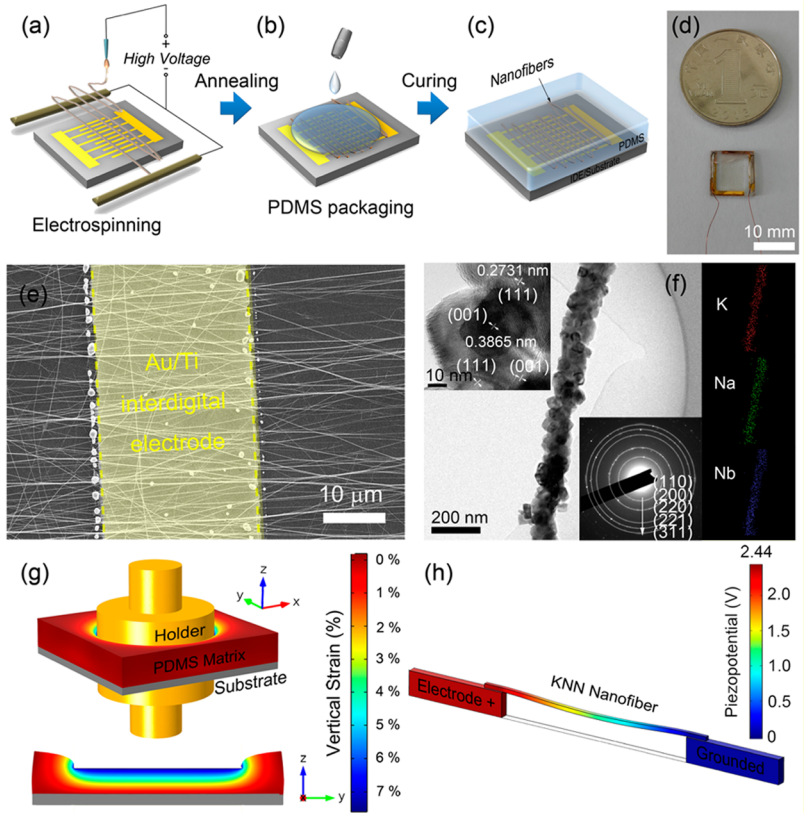

Figure 1. Illustration for the structure and working mechanism of the strain sensor based on laterally aligned KNN nanofibers. (a–c) The schematic diagram of the fabrication procedure and structure of the strain sensor. (d) A photograph of the KNN strain sensor. The spacing of interdigital electrodes was 200 μm. (e) A local SEM image of the strain sensor without the packaging layer. The yellow area represented a stripe of the Au/Ti IDEs. (f) TEM, SAED, HRTEM and EDS-mapping results of an individual KNN nanofiber. (g) The deformation and strain-distribution of the PDMS layer along the out-plane direction obtained through FEA. Two-dimensional picture showing the cross-section view of the strain-distribution from the center face. (h) The distribution of piezopotential generated by the KNN nanofibers lying between the electrodes, which are laterally stretched under the strain of the packaging layers.

based on KNN thin films is comparable to that of $Pb(Zr,Ti)O_3$ (PZT) thin films.[20] Our previous works also demonstrated that the output voltage generated by a single KNN nanorod was much higher than that of individual ZnO nanowires.[21,22] Recently, flexible piezoelectric nanogenerators based on Mn-doped KNN nanofibers was reported by Kang and coauthors.[23] Furthermore, KNN-based materials have already been proven to be biocompatible by Nilsson and co-workers, which are friendly to environment and human bodies for long-term applications.[24,25]

The impact of frequency (strain rate) on sensing behavior is another key issue for piezoelectric active strain sensors. As the electromechanical energy conversion by piezoelectric nanowires is based on the generation of polarization charges under the induced strain, the output voltage/current exhibits switching behavior to the applied force.[26] As a result, active strain sensors are suitable for the measurement of dynamic strains induced by collision, vibration, and other types of unsteady-state forces. According to the piezoelectric theory, the frequency under dynamic conditions is one of the most significant factors to electromechanical conversion efficiency.[27] Therefore, the impact of the frequency should be taken into consideration during the measurement process. The sensing result should be calibrated to increase the accuracy in accordance with the frequency. However, the impact of that and the investigation into the dynamic sensing performance of the piezoelectric active sensors are largely unknown.

In the present work, a self-powered active strain sensor based on well-aligned KNN nanofibers is successfully developed through the electrospinning process on interdigitated electrodes (IDEs). The sensor could generate impulsive output voltage up to 1.6 V to the external circuit under dynamic pressures along the out-plane direction. On the basis of the variation in the amplitude and pulse separation of output voltage signals, both the strain amplitude and vibration frequency can be measured simultaneously without any electrical power input. The relationships between the strain and output voltage are proven to be frequency-dependent. In accordance with the linear correlation between the output voltage and vibration frequency, reliable and accurate sensing results can be obtained after the frequency-calibration.

2. EXPERIMENTAL SECTION

2.1. Electrospinning of KNN Nanofibers. First, the Au/Ti IDEs were fabricated by a standard lift-off photolithography and sputtering process on a cleaned quartz glass substrate. The KNN nanofibers were then assembled on by sol–gel electrospinning and calcination process. The starting precursor for electrospinning was KNN sol–gel, poly(vinylpyrrolidone) (PVP; M_w, 1 300 000) and ethanol. The KNN sol–gel was prepared by using the method reported in our previous work.[28] The KNN sol–gel (0.4 mol/L) was then mixed with the ethanol solution of PVP (0.1 g/mL) and stirred for 5 h to obtain the KNN electrospinning precursor. During the electrospinning process, the KNN precursor was ejected from the syringe pump at a constant rate of 0.25 mL/h. After that, the sample was electrospun

DOI: 10.1021/am5090012
ACS Appl. Mater. Interfaces 2015, 7, 4921–4927

under the electric field of 1.2 kV/cm and collected under a low humidity environment, dried at 80 °C for 5 h, and annealed at 700 °C for 30 min in air. Finally, the sample was packaged by a layer of polydimethylsiloxane (PDMS) matrix after Cu wire leading by conductive Ag paste.

2.2. Finite Element Analysis (FEA). The FEA studies were performed by using 3D steady analysis of piezoelectric module in the COMSOL Multiphysics software. The nanofiber was built as a cuboid with a 100 nm diameter. The parameters for piezoelectric nanofibers were set as piezoelectric constant (d_{33}) of 122 pC/N, relative permittivity (ε_r) of 406, mass density of 7.5 g/cm^3, and elastic compliance constant of 0.96 × 10^{-11} Pa. The packaging PDMS layer was set to be the silicone in the materials library of the software. The electrodes were set as Au with the thickness of 600 μm. The nanofiber was assumed to be in 33 mode for the electromechanical conversion process. Both the nanofiber and silicone were considered isotropic in elastic constants. In addition, the contact potential barrier, external electrical load as well as the conductivity and other parasitic effect of the nanofibers were not considered in this work for simplifying the calculation process. A compressive force of 10^6 N/m^2 was applied on top of the silicone layer, while the bottom side of them was fixed. Moreover, the nanofiber was grounded at one end.

2.3. Characterization and Measurements. The phase and structure of KNN nanofibers were characterized by using X-ray diffraction (XRD, Rigaku SmartLab, Cu Kα, λ = 0.15406 nm). The surface morphology and microstructures of the nanofibers were characterized by using scanning electron microscopy (SEM. JSM6510LV) and transmission electron microscopy (TEM, JEM 2010 with energy dispersive spectrometer, EDS). The electrical signals were recorded by a Keithley 2000 digital multimeter working at the DC voltage mode. The mechanical properties of the device were tested on the dynamic mechanical analyzer (DMA, PerkinElmer Diamond DMA Lab System).

3. RESULTS AND DISCUSSIONS

The schematic diagram of the fabrication process and the structure of the strain sensor are shown in Figure 1a–d. The KNN nanofibers were directly assembled on the prepatterned IDEs (200 μm in spacing) by using a pair of Al stripe as the collector (detailed structure characterization results are shown in Figure S1, Supporting Information). The usage of IDEs increases the defect toleration of the device owing to the parallel connected nanofibers.[29] After the wire-leading, the whole device was packaged by a layer of polydimethylsiloxane (PDMS) as a buffer layer to protect the nanofibers from physical damages. Figure 1e shows the local SEM image of the strain sensor without packaging. The alignment of nanofibers was improved by using the stripe-like collector instead of the conventional flat metal collector (Figure S2, Supporting Information). In this configuration, the direction of electrostatic forces were confined between the stripes, which would lead to the stretching of charged nanofibers in two opposite directions.[30] Based on this understanding, the electromechanical conversion efficiency of the device could be increased due to the enhanced poling efficiency and the strain of nanofibers (Figure S3, Supporting Information). Moreover, TEM results of the as-prepared KNN nanofibers are shown in Figure 1f. The nanofibers with diameter of approximately 100 nm consist of small KNN particles along the axial direction. The selected area electron diffraction (SAED) patterns and high-resolution TEM results confirm that the polycrystalline orthorhombic KNN nanofibers consist of randomly oriented small nanoparticles. Therefore, the nanofibers were first poled by applying a DC voltage of 23 kV/cm on the IDEs before the measurement process.[28] Moreover, the composition of nanofibers was confirmed to be $K_{0.48}Na_{0.52}NbO_3$ according to the EDS results (Figure S4, Supporting Information).

To apply an external pressure to the device for testing the strain sensing performance, we clamped the sensor using a pair of Cu holders. As shown in Figure 1g, the bottom holder was fixed on the stage, while the upper holder was connected to the mechanical linear motor in the dynamic mechanical analyzer (DMA) system. An external pressure was applied on the top surface through the upper holder to induce the vertical strain of the PDMS layer. Under the compression of the PDMS layer, the KNN nanofibers lying on the electrodes were bent along the radical direction. As shown in Figure 1h, the deformation could be considered as a lateral stretching behavior due to the ultrahigh aspect ratio of the nanofibers. Due to the piezoelectric effect, a piezopotential would be generated between both ends of the nanofibers and led to the motion of charge carriers in the external circuit due to the variation of energy barrier at the interface between the electrode and nanofibers.[31] Therefore, the strain of the PDMS layer could be monitored by measuring the output voltage without any electrical power input.

Figure 2 shows the recorded open-circuit voltage signal generated by the strain sensor under the applied periodic

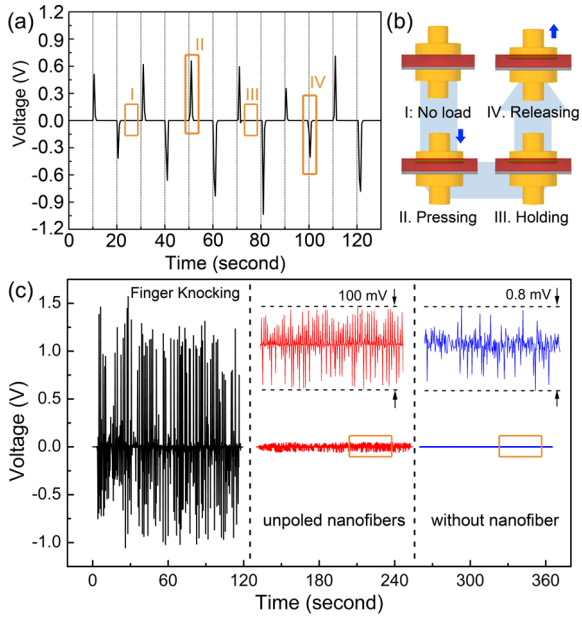

Figure 2. Output voltage of the strain sensor generated by applying the pressures on top of the PDMS layers. (a) Recorded open-circuit voltage signal from the strain sensors with periodic pressure. (b) The action during the periodic measuring process. (c) Recorded open-circuit voltage signal generated by the strain sensor under quick knocking by human fingers. The blue and red curves correspond to the signal generated by the device with no KNN nanofibers and unpoled KNN nanofibers, respectively.

pressure. As shown in Figure 2a,b, the output voltage exhibit obvious switching behavior to the applied pressures. When the PDMS layer was pressed, a positive voltage peak signal was recorded instantly (stage II). However, there was no voltage generated when the pressure was held (stage III). After that, a negative voltage peak was generated by the sensor instantly when the pressure was quickly released (stage IV). This switching behavior is in agreement with the working principle of piezoelectric energy harvesters and suggests that the piezoelectric strain sensor is suitable for detecting the dynamic

DOI: 10.1021/am5090012
ACS Appl. Mater. Interfaces 2015, 7, 4921–4927

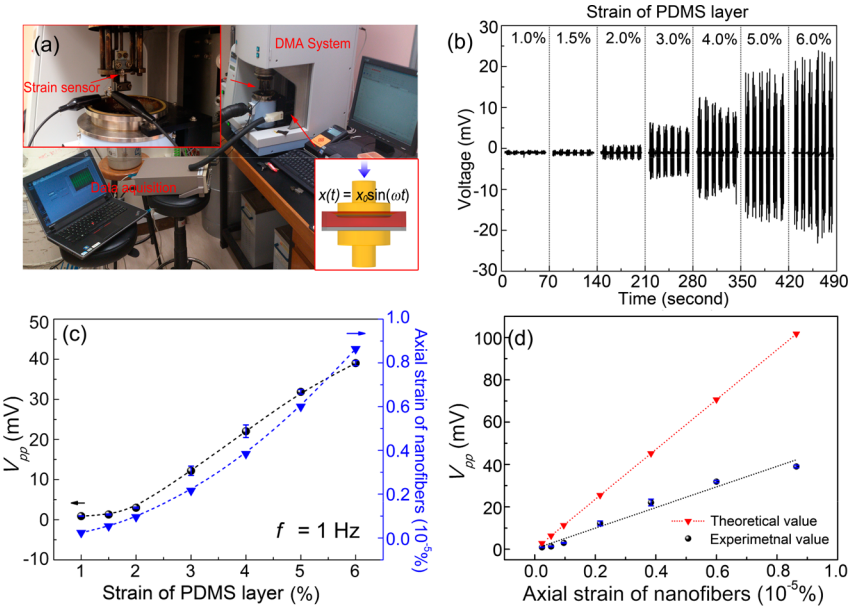

Figure 3. Strain-dependent output voltage of the active strain sensor. (a) The experimental setup of the measurement process; (inset) the mechanical part where the sensor was fixed under the movable holder and connected to the external circuit. (b) The recorded output voltage generated under different strain of PDMS matrix at the fixed frequency of 1 Hz. (c) The relationship between V_{pp} and the strain of PDMS. The blue dot is the calculated value for the axial strain of the nanofibers under different strains applied to the PDMS layer. (d) The theoretical and experimental curve between the strain of KNN nanofiber and V_{pp}.

strains other than the steady ones. Moreover, Figure 2c shows the recorded open-circuit voltage generated by the sensor under a quick knocking on the PDMS layers by human finger. The highest voltage value thus recorded was ~1.6 V, which was comparable to the reported value of PZT nanofibers and much higher than the Mn-doped KNN nanofibers and the parallel connected KNN single-crystalline nanorods in our previous works.[22,23,29] The results also show two controlled experimental results for the devices with no KNN nanofiber and unpoled KNN nanofibers. As shown, the device without KNN nanofibers do not generate obvious electrical output under quick knocking by human fingers, while the devices with unpoled KNN nanofibers generate much lower output voltage (several tens of millivolts) than that with poled nanofibers. The much lower electromechanical conversion efficiency of the unpoled nanofibers should be due to the lower piezoelectric constant without the poling treatment. These results confirm the effect of the poled piezoelectric KNN nanofibers in the sensors. Moreover, the output voltage can be further enhanced either by increasing the spacing of the IDEs (Figure S5, Supporting Information) or through the integration of more rectified sensors in series (Figure S6, Supporting Information). Although the output current is relatively lower (several nA; Figure S7, Supporting Information), the relatively higher output voltage of the nanofibers is sufficient for the active measurement of dynamic strains.[14]

As shown in Figure 3a, a sinusoidal vibration was applied on the top holder along the out-plane direction on the PDMS layers by the DMA system to evaluate the sensor response to dynamic strains. The strain of the PDMS induced by the vibration can be controlled by the DMA system. Figure 3b shows the recorded open-circuit voltage generated by the sensor with the strain varying from 1.0 to 6.0% at the fixed vibration frequency (f = 1 Hz). As shown in Figure 3c, the average peak-to-peak value of the output voltage (V_{pp}) was increased from ~1 to ~40 mV with the increasing strain. This is attributed to the increasing axial strain of the KNN nanofibers below the polymer layer. By assuming that the nanofibers were uniformly bent inside the PDMS layer under input pressure, one can obtain the axial strain of the nanofibers (blue dots in Figure 3c). As shown in Figure 3d, the V_{pp} increases linearly with the axial strain of the nanofibers, which agrees well with the piezoelectric-voltage relationship of the one-dimensional models at steady state (working in 33 mode)[32]

$$V = \int_l Edl = \int_l \frac{d_{33}}{\varepsilon} SYdl \quad (1)$$

where E, d_{33}, ε, S, Y and l are the piezoelectric electrical field, the piezoelectric constant, dielectric constant, axial strain, Young's modulus, and length of the one-dimensional material, respectively. Moreover, the red curve in Figure 3d shows the theoretical value of the peak-to-peak piezopotential generated by the KNN nanofibers in accordance with eq 1. The lower experimental values, compared to those theoretical values, are attributed to the unavoidable disorder in arrangement of nanofibers in the device and the polarization screening effect induced by the free-charge in the material.[33,34]

Figure 4 shows the detailed voltage signal, the strain of the PDMS layers, and the displacement of the top holder with the vibration frequency of 1 Hz. As shown, the strain of the PDMS layer is induced and released only during the first half vibration cycle. After that, the top holder is lifted and detached from the top surface of the PDMS during the other half cycle. As a result, the voltage−time curve is not symmetric, where both of the positive and negative voltage peaks were generated during the first half cycle. It is worth noting that the output voltage is still decreasing after the PDMS is completely released. This phenomenon should be attributed to the incomplete releasing of KNN nanofibers due to the slow rebounding of the PDMS layer. Moreover, because the strain in practical conditions is usually nonperiodic, it is more suitable to evaluate the dynamic strain sensing behavior with strain rate rather than frequency. In

DOI: 10.1021/am5090012
ACS Appl. Mater. Interfaces 2015, 7, 4921−4927

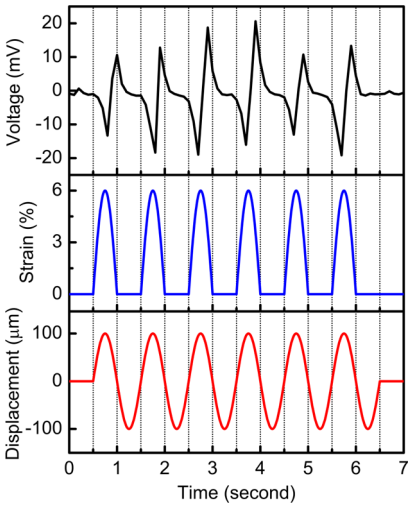

Figure 4. Detailed output voltage signal generated by the strain sensor and the sinusoidal strain and vibration displacement at a fixed frequency of 1 Hz.

accordance with the sinusoidal strain behavior, the time (t_{strain}) for the PDMS to achieve the maximum strain can be obtained as $t_{strain} = (4f)^{-1} = 0.25$ s for vibration frequency of 1 Hz. As a result, the average strain rate for strain of 6% can be calculated as $S/t_{strain} = 24\%/s$, which is corresponding to the axial-strain rate of 3.44×10^{-5} %/s for the KNN nanofibers.

As mentioned above, the impact of the frequency (strain rate) on the sensing performance is a key issue for practical applications. Figure 5a,b shows the output voltage signal generated by the strain sensor when the vibration frequency is changed from 0.2 to 5 Hz at fixed strains of 6.0 and 2.0%, respectively. The results confirm that the output voltage generated by the sensors under the same strain increases linearly with the vibration frequency. As shown in Figure 5c, when the frequency increases from 0.2 to 5.0 Hz at the fixed amplitude, the V_{pp} increases from ~1 to ~25 and from ~8 to ~130 mV under the strains of 2 and 6%, respectively. In addition, the influence of vibration frequency on the sensing behavior can be enhanced at higher strain amplitudes, as suggested by the slope of the red curve (strain = 6%) being higher than that of the black curve (strain = 2%). According to the working principle of piezoelectric energy harvesters, the frequency-dependent sensing behavior could be explained by the fundamental piezoelectric theory. When the axial strain was induced in the nanofibers, the instant current in the external circuit (i_{ex}) would be generated to compensate for the piezopotential induced by the polarization charges. By assuming that there was no leakage current in the device, i_{ex} should be equal to the polarization charges generated by the piezoelectric effect per unit time ($\dot{q}$), which can be represented as

$$i_{ex} = \dot{q} = d_{33}YA\dot{S} \propto d_{33}YASf \quad (2)$$

where A is the cross sectional area, and S is the axial strain of the nanofiber.[35,36] Our experimental results show the agreement where the output voltage (current) increases linearly with the axial strain (frequency) of the nanofiber at certain frequency (axial strain). Therefore, a calibration of the sensing result in accordance with the vibration frequency (strain rate) shall be included. Because the electromechanical conversion behavior of the sensor can be regarded as an instant switching response, the vibration frequency is directly obtained according to the pulse separation of the voltage peaks. For example, in accordance with the detailed profile shown in Figure 5d–f, the pulse separation of responses are calculated as t = 0.5, 0.9, 1.9, and 4.6 s for the input vibration frequency of 2, 1, 0.5, and 0.2 Hz, respectively. These results are consistent with the input parameters during the test process. The small deviations are due to the operation error of the DMA and data acquisition systems. As a result, once a dynamic force is applied on the strain sensor, the induced vibration frequency can be detected. The accurate strain value is then obtained according to the relationship between the output voltage and the strain amplitude at the detected vibration frequency. If the calibration is ignored, one would obtain a different sensing result, for example, the V_{pp} for the strain of 6% at 0.2 Hz, is lower than that for the strain of 2% at 5 Hz. The same process is also

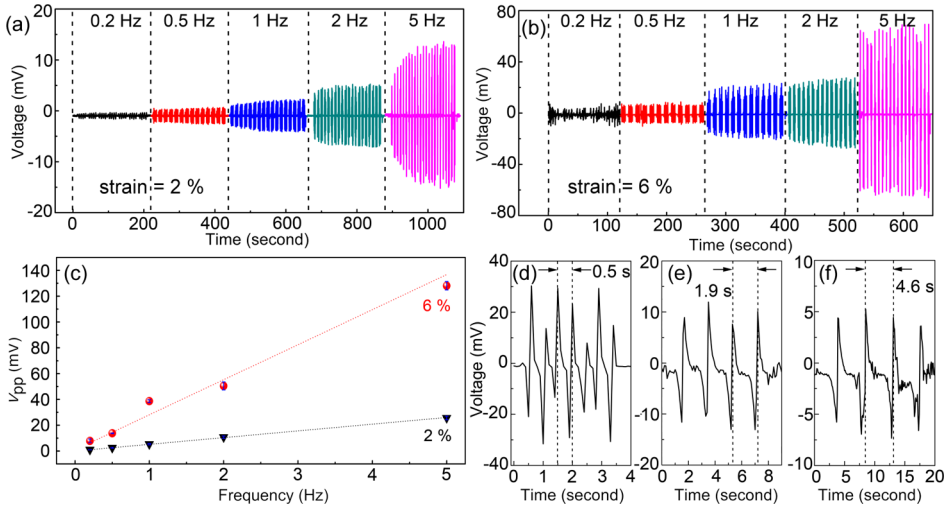

Figure 5. Frequency-dependent output voltage of the strain sensor at the fixed PDMS strains of (a) 6 and (b) 2%. (c) The relationship between the peak-to-peak voltage and the vibration frequency, which can be used for the calibration to the sensing results. The detailed signal for the frequencies of (d) 2, (e) 0.5, and (f) 0.2 Hz are shown for calculating the time intervals.

DOI: 10.1021/am5090012
ACS Appl. Mater. Interfaces 2015, 7, 4921–4927

available for nonperiodic vibration conditions, where one can detect the value of t_{strain} instead of the frequency to realize the calibration to the sensing results (Figures S8–S10, Supporting Information).

4. CONCLUSIONS

A self-powered active strain sensor is successfully developed by using well-aligned lead-free KNN nanofibers synthesized by the electrospinning process. It can generate impulsive voltage of amplitude up to 1.6 V as a result of the nanofiber strain induced by the input vibration on the packaging layer. Therefore, the new device can be used for active sensing of dynamic strains. At a fixed frequency of dynamic strain, the output voltage is increased from ∼1 to ∼40 mV for the strain variation from 1 to 6%, attributed to the piezopotential generated by the nanofibers under axial strain condition. Our results also confirm that the vibration frequency (time for achieve the maximum strain) can be measured by the pulse separation of the voltage peaks during the sensing process. The frequency greatly impacts the sensing behavior of KNN nanofibers. The output voltage is increased by an order of magnitude when the input frequency increases from 0.2 to 5 Hz. As a result, the sensing result will need to be calibrated in accordance with the frequency by synchronously monitoring the strain amplitude and vibration frequency.

■ ASSOCIATED CONTENT

Supporting Information

X-ray diffraction spectra; scanning electron microscopy; energy dispersive spectrum; finite element analysis results; and output performance of the devices with increased IDE spacing, rectifying, and integration; as well as the detailed voltage signal for calibration. This material is available free of charge via the Internet at http://pubs.acs.org.

■ AUTHOR INFORMATION

Corresponding Authors

*E-mail: guhsh@hubu.edu.cn.
*E-mail: apywang@polyu.edu.hk.

Author Contributions

The manuscript was written through contributions of all authors. All authors have given approval to the final version of the manuscript.

Notes

The authors declare no competing financial interest.

■ ACKNOWLEDGMENTS

The authors thank Prof. Yang Luo of the East China Normal University for the discussion about the finite element analysis works. This work was financially supported by the National Science Foundation of China (Grant Nos. 11474088, 61274073), the National High-Tech Research and Development Program of China (863 Program, Grant No. 2013AA031903), the Applied Basic Research Project of Wuhan (Grant No. 2014010101010006), and the Natural Science Foundation of Hubei Province in China (Grant No. 2014CFB557).

■ REFERENCES

(1) Wang, Z.; Qi, J.; Yan, X.; Zhang, Q.; Wang, Q.; Lu, S.; Lin, P.; Liao, Q.; Zhang, Z.; Zhang, Y. A Self-Powered Strain Senor Based on a ZnO/PEDOT:PSS Hybrid Structure. *RSC Adv.* **2013**, *3*, 17011–17015.

(2) Lin, L.; Wang, S.; Niu, S.; Liu, C.; Xie, Y.; Wang, Z. L. Noncontact Free-Rotating Disk Triboelectric Nanogenerator as a Sustainable Energy Harvester and Self-Powered Mechanical Sensor. *ACS Appl. Mater. Interfaces* **2014**, *6*, 3031–3038.

(3) Bai, P.; Zhu, G.; Jing, Q.; Yang, J.; Chen, J.; Su, Y.; Ma, J.; Zhang, G.; Wang, Z. L. Membrane-Based Self-Powered Triboelectric Sensors for Pressure Change Detection and Its Uses in Security Surveillance and Healthcare Monitoring. *Adv. Funct. Mater.* **2014**, *24*, 5807–5813.

(4) Zhang, H.; Yang, Y.; Su, Y.; Chen, J.; Adams, K.; Lee, S.; Hu, C.; Wang, Z. L. Triboelectric Nanogenerator for Harvesting Vibration Energy in Full Space and as Self-Powered Acceleration Sensor. *Adv. Funct. Mater.* **2014**, *24*, 1401–1407.

(5) Lin, L.; Hu, Y.; Xu, C.; Zhang, Y.; Zhang, R.; Wen, X.; Lin Wang, Z. Transparent Flexible Nanogenerator as Self-Powered Sensor for Transportation Monitoring. *Nano Energy* **2013**, *2*, 75–81.

(6) Yang, Y.; Guo, W.; Qi, J.; Zhang, Y. Flexible Piezoresistive Strain Sensor Based on Single Sb-Doped ZnO Nanobelts. *Appl. Phys. Lett.* **2010**, *97*, 223117.

(7) Zhao, J.; He, C.; Yang, R.; Shi, Z.; Cheng, M.; Yang, W.; Xie, G.; Wang, D.; Shi, D.; Zhang, G. Ultra-Sensitive Strain Sensors Based on Piezoresistive Nanographene Films. *Appl. Phys. Lett.* **2012**, *101*, 063112.

(8) Wang, B.; Lee, B.-K.; Kwak, M.-J.; Lee, D.-W. Graphene/Polydimethylsiloxane Nanocomposite Strain Sensor. *Rev. Sci. Instrum.* **2013**, *84*, 105005.

(9) Wu, J. M.; Chen, K.-H.; Zhang, Y.; Wang, Z. L. A Self-Powered Piezotronic Strain Sensor Based on Single $ZnSnO_3$ Microbelts. *RSC Adv.* **2013**, *3*, 25184–25189.

(10) Aifang, Y.; Yong, Z.; Peng, J.; Zhong Lin, W. A Nanogenerator as a Self-Powered Sensor for Measuring the Vibration Spectrum of a Drum Membrane. *Nanotechnology* **2013**, *24*, 055501.

(11) Hu, Y.; Xu, C.; Zhang, Y.; Lin, L.; Snyder, R. L.; Wang, Z. L. A Nanogenerator for Energy Harvesting from a Rotating Tire and Its Application as a Self-Powered Pressure/Speed Sensor. *Adv. Mater.* **2011**, *23*, 4068–4071.

(12) Zhang, R.; Lin, L.; Jing, Q.; Wu, W.; Zhang, Y.; Jiao, Z.; Yan, L.; Han, R. P. S.; Wang, Z. L. Nanogenerator as an Active Sensor for Vortex Capture and Ambient Wind-Velocity Detection. *Energy Environ. Sci.* **2012**, *5*, 8528–8533.

(13) Lee, J.; Choi, B. Development of a Piezoelectric Energy Harvesting System for Implementing Wireless Sensors on the Tires. *Energy Convers. Manage.* **2014**, *78*, 32–38.

(14) Lin, L.; Jing, Q.; Zhang, Y.; Hu, Y.; Wang, S.; Bando, Y.; Han, R. P. S.; Wang, Z. L. An Elastic-Spring-Substrated Nanogenerator as an Active Sensor for Self-Powered Balance. *Energy Environ. Sci.* **2013**, *6*, 1164–1169.

(15) Wang, Z. L.; Song, J. Piezoelectric Nanogenerators Based on Zinc Oxide Nanowire Arrays. *Science* **2006**, *312*, 242–246.

(16) Wang, X.; Song, J.; Liu, J.; Wang, Z. L. Direct-Current Nanogenerator Driven by Ultrasonic Waves. *Science* **2007**, *316*, 102–105.

(17) Yang, R.; Qin, Y.; Dai, L.; Wang, Z. L. Power Generation with Laterally Packaged Piezoelectric Fine Wires. *Nat. Nanotechnol.* **2009**, *4*, 34–39.

(18) Coondoo, I.; Panwar, N.; Kholkin, A. Lead-Free Piezoelectrics: Current Status and Perspectives. *J. Adv. Dielectr.* **2013**, *03*, 1330002.

(19) Egerton, L.; Dillon, D. M. Piezoelectric and Dielectric Properties of Ceramics in the System Potassium—Sodium Niobate. *J. Am. Ceram. Soc.* **1959**, *42*, 438–442.

(20) Kanno, I.; Ichida, T.; Adachi, K.; Kotera, H.; Shibata, K.; Mishima, T. Power-Generation Performance of Lead-Free (K,Na)-NbO_3 Piezoelectric Thin-Film Energy Harvesters. *Sens. Actuators, A* **2012**, *179*, 132–136.

(21) Wang, Z.; Gu, H.; Hu, Y.; Yang, K.; Hu, M.; Zhou, D.; Guan, J. Synthesis, Growth Mechanism and Optical Properties of (K,Na)NbO_3 Nanostructures. *CrystEngComm* **2010**, *12*, 3157–3162.

(22) Wang, Z.; Hu, Y.; Wang, W.; Zhou, D.; Wang, Y.; Gu, H. Electromechanical Conversion Behavior of $K_{0.5}Na_{0.5}NbO_3$ Nanorods

DOI: 10.1021/am5090012
ACS Appl. Mater. Interfaces 2015, 7, 4921–4927

Synthesized by Hydrothermal Method. *Integr. Ferroelectr.* **2013**, *142*, 24−30.
(23) Kang, H. B.; Chang, J.; Koh, K.; Lin, L.; Cho, Y. S. High Quality Mn-Doped (Na,K)NbO_3 Nanofibers for Flexible Piezoelectric Nanogenerators. *ACS Appl. Mater. Interfaces* **2014**, *6*, 10576−10582.
(24) Nilsson, K.; Lidman, J.; Ljungstrom, K.; Kjellman, C. Biocompatible Material for Implants. U.S. Patent, 6526984, March 4, 2003.
(25) Jalalian, A.; Grishin, A. M. Biocompatible Ferroelectric (Na,K)NbO_3 Nanofibers. *Appl. Phys. Lett.* **2012**, *100*, 012904.
(26) Wang, Z. L. Towards Self-Powered Nanosystems: From Nanogenerators to Nanopiezotronics. *Adv. Funct. Mater.* **2008**, *18*, 3553−3567.
(27) Sirohi, J.; Chopra, I. Fundamental Understanding of Piezoelectric Strain Sensors. *J. Intell. Mater. Syst. Struct.* **2000**, *11*, 246−257.
(28) Zhou, D.; Gu, H.; Hu, Y.; Tian, H.; Wang, Z.; Qian, Z.; Wang, Y. Synthesis, Characterization and Ferroelectric Properties of Lead-Free $K_{0.5}Na_{0.5}NbO_3$ Nanotube Arrays. *J. Appl. Phys.* **2011**, *109*, 114104.
(29) Chen, X.; Xu, S.; Yao, N.; Shi, Y. 1.6 V Nanogenerator for Mechanical Energy Harvesting Using PZT Nanofibers. *Nano Lett.* **2010**, *10*, 2133−2137.
(30) McCann, J. T.; Chen, J. I. L.; Li, D.; Ye, Z.-G.; Xia, Y. Electrospinning of Polycrystalline Barium Titanate Nanofibers with Controllable Morphology and Alignment. *Chem. Phys. Lett.* **2006**, *424*, 162−166.
(31) Wang, Z. L.; Yang, R.; Zhou, J.; Qin, Y.; Xu, C.; Hu, Y.; Xu, S. Lateral Nanowire/Nanobelt Based Nanogenerators, Piezotronics and Piezo-Phototronics. *Mater. Sci. Eng., R* **2010**, *70*, 320−329.
(32) Chen, X.; Xu, S.; Yao, N.; Xu, W.; Shi, Y. Potential Measurement from a Single Lead Ziroconate Titanate Nanofiber Using a Nanomanipulator. *Appl. Phys. Lett.* **2009**, *94*, 253113.
(33) Xue, X.; Nie, Y.; He, B.; Xing, L.; Zhang, Y.; Wang, Z. L. Surface Free-Carrier Screening Effect on the Output of a ZnO Nanowire Nanogenerator and Its Potential as a Self-Powered Active Gas Sensor. *Nanotechnology* **2013**, *24*, 225501.
(34) Hu, Y.; Lin, L.; Zhang, Y.; Wang, Z. L. Replacing a Battery by a Nanogenerator with 20 V Output. *Adv. Mater.* **2012**, *24*, 110−114.
(35) Agrawal, R.; Peng, B.; Espinosa, H. D. Experimental−Computational Investigation of ZnO Nanowires Strength and Fracture. *Nano Lett.* **2009**, *9*, 4177−4183.
(36) Zhu, G.; Yang, R.; Wang, S.; Wang, Z. L. Flexible High-Output Nanogenerator Based on Lateral ZnO Nanowire Array. *Nano Lett.* **2010**, *10*, 3151−3155.

DOI: 10.1021/am5090012
ACS Appl. Mater. Interfaces 2015, 7, 4921−4927